Journal of Materials Chemistry B

Accepted Manuscript

ROYAL SOCIETY OF CHEMISTRY

www.rsc.org/materialsB

Cite this: DOI: 10.1039/c0xx00000x

www.rsc.org/xxxxxx

ARTICLE TYPE

Undecylprodigiosin conjugated monodisperse gold nanoparticles efficiently cause apoptosis in colon cancer cells *in vitro*

Jasmina Nikodinovic-Runic,[a#] Marija Mojic,[b#] Yijin Kang,[c#] Danijela Maksimovic-Ivanic,[b] Sanja Mijatovic,[b] Branka Vasiljevic,[a] Vojislav R Stamenkovic*[c] and Lidija Senerovic*[a]†

Received (in XXX, XXX) XthXXXXXXXXX 20XX, Accepted Xth XXXXXXXXX 20XX
DOI: 10.1039/b000000x

Bacterial pigment undecylprodigiosin (UP) was produced using *Streptomyces* sp. JS520 and conjugated to monodisperse gold nanoparticles (UP-Au). Both UP and UP-Au showed cytocidal activity towards melanoma (A375), lung carcinoma (A549), breast cancer (MCF-7) and colon cancer (HCT-116) cells, inducing apoptosis with IC_{50} values ranging from 0.4 to 4 μg/ml. Unconjugated UP had tendency to lose its activity over time and to change biophysical characteristics over pH. The loss of the pigment potency was overcome by conjugation with gold nanoparticles. UP-Au exhibited high stability over pH 3.8 to 7.4 and its activity remained unaffected in time. Nano-packing changed the mechanism of UP toxicity by converting the intracellular signals from mitochondrial dependent to mitochondrial independent apoptotic process. Availability of nonpyrogenic UP in high amounts, together with specific anticancer activity and improved stability in the complex with gold nanoparticles present a novel platform for further development of UP-Au complexes as an anticancer drug suitable for clinical applications.

1 Introduction

Cancer is one of the deadliest diseases worldwide with lung and colorectal cancers ranking the first and the third most common cancer types.[1] Cancer attracts global attention in the quest to define novel therapies based on understanding of the mechanisms that induce this disorder as well as on the ability to address key obstacles in available treatments. For instance, critical issues of conventional chemotherapy are high toxicity, lack of selectivity and restricted drug accessibility to the cancer tissue.[1] Even if the drugs reach the cancer cells, multidrug resistance (MDR) represents significant obstacle that emerges during the therapy.[2]Therefore, the continuous effort aimed towards more efficient drugs either via increased specificity or targeted delivery to cancer cells is of paramount importance.

Natural products such as secondary metabolites of microorganisms, animals and plants have demonstrated less toxicity than synthetic compounds used currently for the cancer treatments, and therefore, present a promising approach for the development of the novel drugs.[3] Tripyrrole bacterial red pigment family including 2-methyl-3-phentyl-6-methoxyprodigiosene (PG), cycloprodigiosin (cPrG), nonylprodigiosin, metacycloprodigiosin, and undecylprodigiosin (prodigiosin 25-C, UP) have been recently in focus of anticancer drug development.[4] Prodigiosin family members (including UP) show numerous biological activities including antibacterial, antifungal, antimalarial, immunosuppressive, as well as anticancer.[4-7] Like other family members, UP can have multiple cellular targets and employ different molecular mechanisms to induce apoptosis in cancer cells. However, anticancer properties of UP have not been thoroughly investigated. Up to date *in vitro* activity of UP was reported against mouse and human leukemia, human hepatic carcinoma, human lung carcinoma[8, 9] while p53 independent apoptosis was demonstrated in breast cancer cells.[10] Cancer specificity and p53 independent toxicity make UP an excellent candidate for further examination of its functional properties.

In addition to novel class of anti cancer compounds their efficiency, selectivity and targeted delivery could be substantially enhanced by proper selection of a drug carrier. A great potential for such improvements in cancer therapy lies in utilization of nanoscalematerials.[11-13] The synergy between nanomaterials and anticancer compounds presents compelling approach for the development of the drug-delivery scaffolds.[14] As an example, gold nanoparticles are known to be nontoxic, nonimmunogenic[15, 16], and can be easily functionalized with one or multiple molecules of interest.[17-20] Depending on the size and biophysical properties, gold nanoparticles have the ability to improve stability of small molecules, their water solubility and to enable specific delivery of the drug to the cancer cells thus declining the side effects of the drugs.[21-24] Moreover, the binding of the small molecules to gold nanoparticles can decrease its efflux from the cancer cells reducing the effect of multi drug resistance.[25-28] The anticancer agents that were successfully conjugated to gold nanoparticles include paclitaxel[29], tamoxifen[30], gemcitabine[17] and oxaliplatin.[31] Doxorubicin, a secondary metabolite of *Streptomyces peucetius* ATCC 27952, very potent anticancer agent was stabilized through conjugation to Au nanoparticles.[26, 32] The nano-packing resulted in increased water solubility and

excellent pH responsive drug release.[26]

We have recently described UP producing strain *Streptomyces* sp. JS520 and showed its antimicrobial, UV protective and antioxidative activity.[7] In this study we produced high amounts of UP by *Streptomyces* sp. JS520 and report its potent activity against spectrum of cancer cell lines including aggressive colon cancer. Conjugation of UP to gold nanoparticles has been employed to obtain novel material with improved chemotherapeutic properties. The mechanism of cytotoxicity of both, the pure and Au conjugated pigment (UP-Au) is assessed and explained.

2 Experimental section

2.1 Production and purification of undecylprodigiosin (UP)

Undecylprodigiosin (UP) was synthesized in shake flask culture of *Streptomyces* sp. JS520 using mannitol-soy-yeast medium supplemented with methyl-oleate (0.2%, v/v) for 6 days at 30°C and recovered and purified by column chromatography as described previously.[7] The quality of the purified UP was analyzed by liquid chromatography coupled to mass spectroscopy (LC-MS).[7]

2.2 Synthesis and conjugation of UP-Au nanoparticles

The Au nanoparticles were synthesized following the procedure described in the literature.[33] Briefly, 1 mmol (≈0.4 g) $HAuCl_4 \cdot 3H_2O$ was dissolved in toluene (50 ml) containing oleylamine (5 ml). The solution was then heated to and kept at 70-75°C for 24 h until red color developed indicating the formation of Au nanoparticles. Ethanol (100 ml) was added to the suspension, and Au nanoparticles were collected by centrifugation at 7,000 rcf at 25°C for 3 min. Size selective precipitation was employed to purify Au nanoparticles and to select nanoparticles of desired size, as described in literature.[34, 35]

Conjugation of UP to Au nanoparticles was achieved by ligand-exchange. Prepared Au nanoparticles (capped with oleylamine) were mixed with UP solution at the ratio of at least 0.1 mmol UP/mg Au, and heated at 60°C with stirring for 24 h. UP-Au were collected by centrifugation (11000 rcf, 25°C, 10 min.), and were characterized by Transmission electron microscope (TEM, FEI CM30T; Field Emission Inc., Oregon, USA), Fourier transform infrared spectroscopy (FT-IR), Raman spectroscopy (Renishaw, 633 nm light source), and thermogravimetric analysis (TGA).

2.3 *In vitro* stability of UP and UP-Au nanoparticles

The stability of UP and UP-Au was examined in four different buffers: 50 mM HEPES, pH 7.4, 50 mM MES, pH 6.2, 50 mM Glycine-HCl, pH 4.4 and 3.8. All buffers contained 120 mMNaCl and 20% (w/v) foetal bovine serum (FBS) (Sigma, Munich, Germany). UP (10 µg/ml) was incubated for 24, 48 and 72 h and the stability was assessed by UV-Vis spectroscopy. The UV-Vis spectra were recorded at 200- 700 nm at 0.5 nm intervals by UV/Visible spectrophotometer Ultrospec 3300pro (Biochrom, Cambridge, UK).

The release of UP from Au nanoparticles was analyzed after incubation of UP-Au in the same buffers as above. 110 µg/ml UP- Au nanoparticles was added to 2 ml of buffer and incubated for 24, 48 and 72 h at room temperature. The samples were centrifuged at 50,000 rcf for 20 min (Beckman Optima^{TM}L-80 XP Ultracentrifuge, Beckman Coulter, CA, USA) and the presence of UP released from the complex in the supernatant was measured by UV-Vis spectroscopy (Ultrospec 3300pro; Biochrom, Cambridge, UK). The UP-Au nanoparticles in buffer solutions were also examined by Raman spectroscopy (Renishaw, 633 nm light source) to assess the stability at various pH values.

2.4 Cell culture

Colon cancer cell line (HCT-116) and melanoma (A375) were donated from Prof.FerdinandoNicoletti (Department of Biomedical Sciences, University of Catania, Italy). Lung carcinoma (A549) and breast cancer (MCF-7) cell lines were obtained from the American Type Culture Collection (ATCC). Cells were maintained as monolayer cultures in RPMI-1640 supplemented with 100 µg/ml streptomycin, 100 U/ml penicillin and 10% (v/v) FBS (all from Sigma, Munich, Germany). All cells were grown in humidified atmosphere of 95% air and 5% CO_2 at 37°C.

2.5 MTT and crystal violet cell (CV) viability assays

The viability of cells was evaluated with 3-(4,5-dimethylthiazol-2-yl)-2,5-diphenyltetrazolium bromide (MTT) and crystal violet (CV). Assays were carried out after 48 h of cell incubation in the media containing test compounds at different concentrations and the viability was measured as described.[36] The results are presented as percentage of the control (untreated cells) that was arbitrarly set to 100%.

2.6 Lactate dehydrogenase (LDH) release assay

For determination of LDH release, cells were cultivated in phenol red free medium for 48 h in the presence of different doses of tested compounds and assay was performed as described previously.[37]

2.7 Cell cycle analysis

Cells (2.5 x 10^5 per well) were treated with IC_{50} doses of each compound for 48 h, then trypsinized and fixed in 70% (v/v) ethanol at 4°C for 30 min. After washing in PBS, cells were incubated with propidium iodide (PI, Molecular Probes, Invitrogen, Carlsbad, CA) (20 mg/ml) and RNase (0.1 mg/ml) for 45 min at 37°C in dark. Red fluorescence was analysed with CyFlow® Space Partec (Partec GmbH, Munster, Germany). The distribution of cells in different cell cycle phases was determined with PartecFloMax® software (Partec GmbH, Munster, Germany).

2.8 Propidium iodide (PI) and AnnexinV-FITC/PI staining of cells

Cells (1 x 10^4 per well) were treated with IC_{50} dose of each compound for 24 h, then PI staining was performed as described above. The cells were visualized by Zeiss Axiovert microscope (Carl Zeiss GmbH, Vienna, Austria).

Cells (2.5 x 10^5 per well) were treated with IC_{50} doses of each compound for 48 h, then trypsinized and stained with AnnexinV-FITC/PI (Molecular Probes, Invitrogen, Carlsbad, CA). Cells were analyzed with a CyFlow® Space Partec using PartecFloMax® software (Partec GmbH, Munster, Germany).

2.9 Caspase detection

Cells (2.5 x 10^5 per well) were treated with IC_{50} doses of each compound for 48 h, then trypsinized and stained with apostat (R&D Systems, Minneapolis, MN, USA) in phenol red free RPMI supplemented with 15 % FCS for 30 min at 37°C. After washing, cells were analysed with the CyFlow® Space Partec using PartecFloMax® software (Partec GmbH, Munster, Germany).

2.10 JC-1 staining

Staining of cells (2.5 x 10^5 per well treated with IC_{50} doses of each compound for 48 h) with lipophilic cationic probe 5,5′,6,6′-tetrachloro-1,1′,3,3′-tetraethylbenzimidazolcarbocyanine iodide (JC-1) was carried out to determine mitochondrial membrane potential changes according to the published procedure.[38]

2.11 Immunostaining

At indicated time points, cells were lysed in protein lysis buffer containing 62.5 mM Tris-HCl (pH 6.8 at 25°C), 2% (w/v) SDS, 10% (v/v) glycerol, 50 mM dithiothreitol, and 0.01% (w/v) bromphenol blue and subjected to electrophoresis on 12% (w/v) SDS-polyacrylamide gels. Electrotransfer to polyvinylidene difluoride membranes at 5 mA/cm^2 was done using a semidry blotting system (Fastblot B43; Bio-Rad, Goettingen, Germany). The membranes were blocked with 5% (w/v) nonfat dry milk in PBS with 0.1% (v/v) Tween 20, and then blots were incubated with specific antibodies to selection of pro- and antiapoptotic proteins Bim, Smac/DIABLO (eBioscience, CA, USA), XIAP (Cell Signaling Technology, Danvers, MA) and actin (Santa Cruz Biotechnology, Inc., CA, USA), followed by incubation with secondary antibody (ECL donkey anti-rabbit horseradish peroxidase-linked; GE Healthcare, Chalfont St. Giles, Buckinghamshire, UK). Bands were visualized using a chemiluminescence detection system (ECL; GE Healthcare, Chalfont St. Giles, Buckinghamshire, UK).

Statistical analysis. For the statistical analysis, we used a *t*-test to compare values between two groups. Differences were defined as significant at $p<0.05$.

3 Results and discussion

3.1 Synthesis and characterization of UP and UP-Au nanoparticles

Pure undecylprodigiosin (UP; Fig. 1A) was obtained by bacterial fermentation from cultures of *Streptomyces* sp. JS520 in high yields (130 mg/l). UP was recovered from the culture by standard solvent extraction followed by silica column chromatography and the spectral data of the obtained product was in good agreement with those reported in literature for UP.[7, 39, 40]

The pigment was conjugated to gold nanoparticles (Fig. 1B) to examine the suitability of the approach for further development of its therapeutic properties. It is well established that size of the nanoparticles influences their *in vivo* performance.[11, 41] Nanoparticles of 5 nm and below are cytotoxic and when applied intravenously are easily cleared from the blood stream and are excreted via urine.[42] Although larger nanoparticles (20 – 100 nm) may provide specific tissue delivery [22, 43], we have chosen monodisperse Au nanoparticles of 5 – 10 nm for their ability to escape uptake by mononuclear phagocytic cells and to utilize enhanced permeation and retention effect in solid tumor tissue.[43, 44] The synthesis of monodisperse Au nanoparticles with a size below 5 nm has been well developed.[45-47] However, current methods to produce Au nanoparticles at the size range of 5-20 nm usually generate particles over a broad size distribution and the efficient method to achieve monodispersity is still to be established. We have employed a post-treatment of size selective precipitation to select the Au nanoparticles of the desired size (between 5-10 nm). Upon standard preparation obtained Au nanoparticles had a broad size distribution from 3-12 nm (average size of 8.0 nm, σ = 22%) (Fig. 1C). After the size selective precipitation, which was aimed to cut off the portion of small particles, the size distribution was significantly narrowed (average size of 8.5 nm, σ = 9%) (Fig. 1D).

The efficient conjugation of UP to uniform Au nanoparticles was achieved by ligand exchange through chemical equilibrium as confirmed by FT-IR spectral analysis (Fig. 1E and 1F). The adsorption of UP and desorption of oleylamine was achieved by keeping the population of UP substantially higher (by 100 times) than that of oleylamine.The peak seen in the oleylamine spectrum around 3300 cm^{-1} was ascribed to symmetric stretching vibration of NH_2,[48] which does not exist in UP molecule. In the IR-fingerprint region (500-1500 cm^{-1}), which is highlighted in Fig. 1E and shown in Fig. 1F, the spectrum of UP-Au is distinguished from that of oleylamine but similar to that of UP, confirming the successful exchange of oleylamine ligands to UP molecules.Furthermore, TGA data showed that after heating Au nanoparticles to 600°C 72.3% mass remained, implying approximately 1 μm ololeylamine molecules were attached to 1 mg of Au nanoparticles. After the ligand exchange, the remaining mass was 90.8%, corresponding to 0.25 μmol UP molecules per mg Au nanoparticles (Supporting Information, Fig. S1). Considering the steric effect from the bulky head group of pyrrole and that each UP molecule has two NH bonds which may be attached to the Au nanoparticle (Fig. 1A and 1B), it is expected that the population of UP attached on each Au nanoparticle should be smaller than that of oleylamine which is in a good agreement with TGA data. This was also implied by FT-IR data, in which C-H stretching vibration peaks at 2920 cm^{-1} and 2850 cm^{-1} showed stronger intensities on spectrum of oleylamine capped Au nanoparticles than on that of UP capped Au nanoparticles. Although there is no efficient method that would enable complete ligand exchange, our data suggest that at least the majority of oleylamine ligands were successfully replaced by UP molecules, achieving the UP-Au conjugation.

3.2 Stability of UP and UP-Au nanoparticles

It has been reported that prodigiosins are pH sensitive, being stable in acidic but unstable in alkaline pH environments.[49, 50] Therefore, the stability of UP and UP-Au conjugate was tested by prolonged incubation (72 h) in buffers at four different pH values. Buffers were prepared with FCS 20% (v/v) in order to mimic physiological conditions. The change was observed in absorption spectra of all UP solutions (pH 3.8, 4.4, 6.8 and 7.4) with the new defined absorption maxima appearing at 430 nm and the characteristic UP absorption maxima peak (535 nm) decreasing (Fig. 2).

Cite this: DOI: 10.1039/c0xx00000x

www.rsc.org/xxxxxx

ARTICLE TYPE

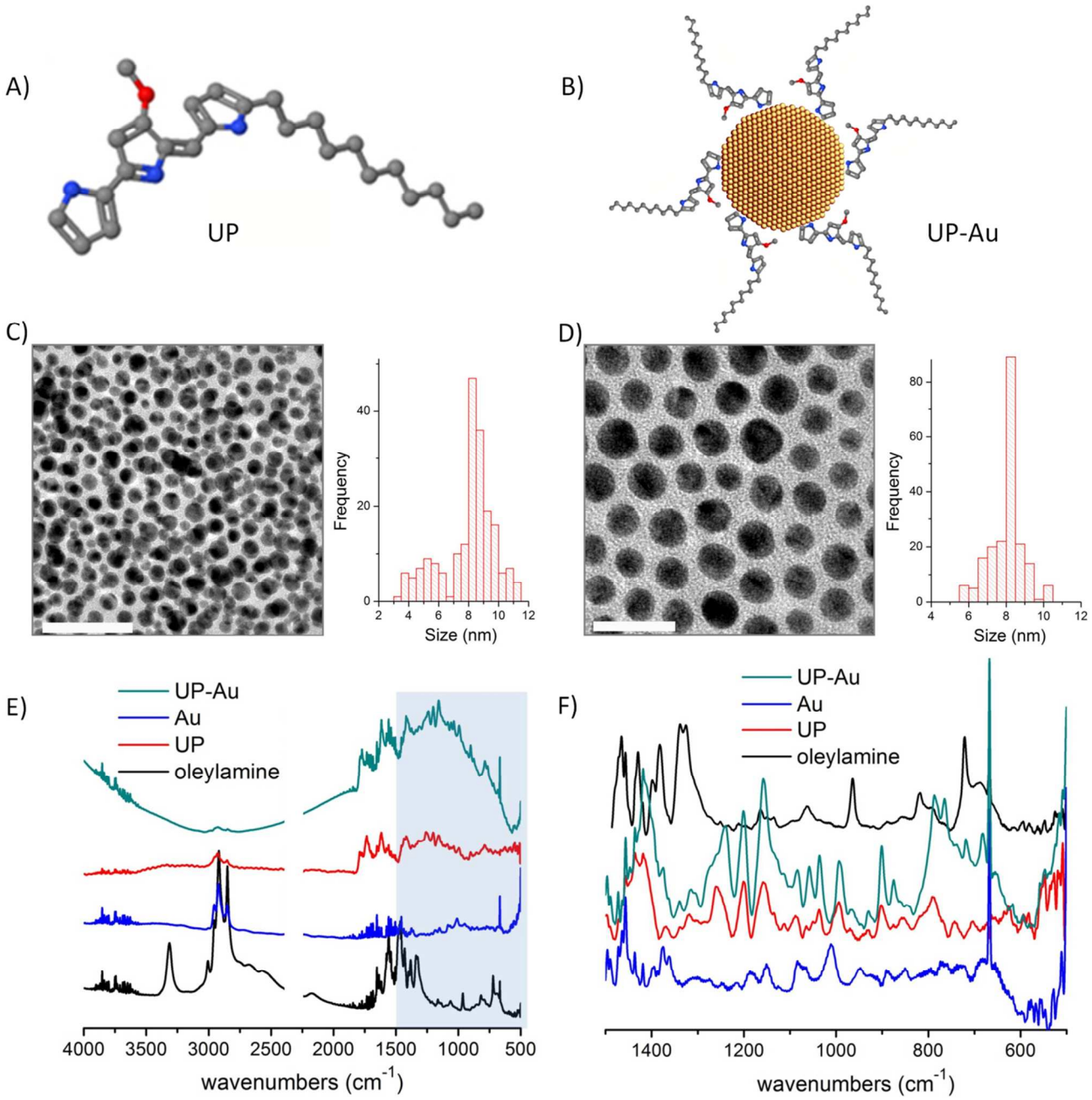

Fig.1 Undecylprodigiosin (A) and UP-Au conjugate (B) (nitrogen, oxygen, carbon and gold atoms are presented with blue, red, grey and yellow colours respectively). TEM images and histograms of Au nanoparticles C) as-synthesized and D) size selective precipitation processed. Histograms are based on 200 counts. E) FT-IR spectra of conjugated UP-Au nanoparticles, oleylamine-capped Au nanoparticles, UP molecules and oleylamine molecules. F) Fingerprint region of FT-IR spectra corresponding to the highlighted region in E.

Due to the specific pyrrydipyrrylmethene structure and good electron transportability UP can interfere with multiple cellular processes and react with different biomolecules.[49, 51] On the other side its chemical characteristics can result in the pigment instability at physiological pH. This effect was not observed in the case of UP-Au conjugate as nano-preparation did not have defined absorption spectra (data not shown). Solutions of UP-Au were ultracentrifuged and the release of the pigment from the gold nanoparticles was examined using UV-Vis spectroscopy. The binding of UP to Au was stable at all pH values tested since

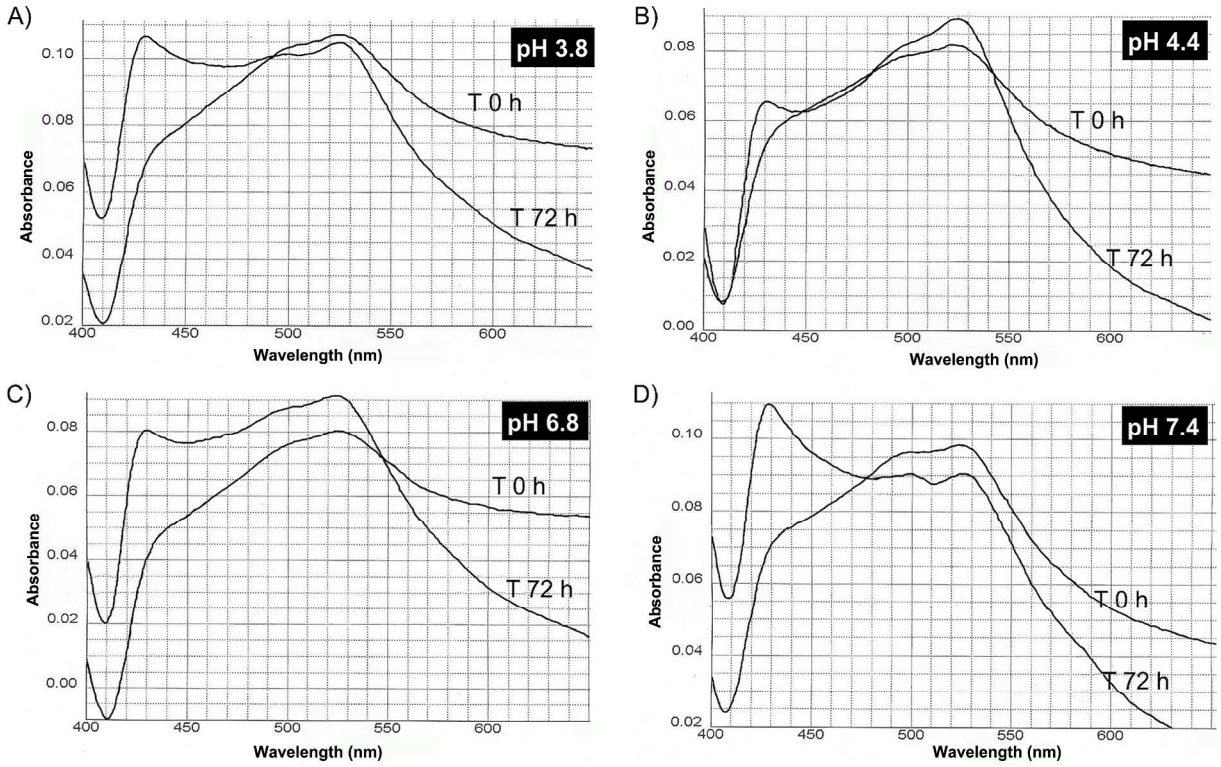

Fig.2 Changes absorption spectra of UP dissolved in Glycine-HCl buffer pH 3.8 (A), Glycine-HCl buffer pH 4.4 (B) MES buffer pH 6.2 (C) and HEPES buffer pH 7.4 (D) upon incubation for 72 h at room temperature.

no pigment was detected in the supernatant after ultracentrifugation (data not shown).

The stability of UP and UP-Au conjugate was also tested by Raman spectroscopy (Fig. 3). The small signature peak of Au nanoparticles was observed at 2920 cm^{-1}, while peaks with strong intensities were ascribed to the surface enhanced Raman scattering (SERS), indicating the interaction between Au and UP molecules. After prolonged incubation for 72 h, the peaks corresponding to SERS remain, suggesting that the UP-Au is stable at various pH values. Noteworthy, the SERS peaks seen at pH of 6.8 (Fig. 3C) and 7.4 (Fig. 3D) are not as strong as those seen at pH of 3.8 (Fig. 3A) and 4.4 (Fig. 3B), implying the UP-Au conjugate is more stable in acid environment.

Recently, Au nanoparticles were used as cisplatin drug delivery vehicles and significant improvement of stability over time was reported.[52] Cisplatin was conjugated through poly (ethylene glycol) linker and monodispersity and reproducibility of nanoparticles preparation were identified as critical parameters. In our work monodispersity was achieved by size selective precipitation step (Fig. 1D) and similarly to results described by Craig and co-authors [52] stabilization of UP over time and pH was achieved (Fig. 2 and 3).

3.3 *In vitro* cytotoxicity and anticancer activity of UP and UP-Au conjugated nanoparticles

The cancer specific activity of prodigiosins has been well documented on approximately 60 different cancer cell lines.[53,4] UP was the least studied prodigiosin family member most likely due to the limited amount of the available pigment. Although produced in a relatively high yield by *Serratia marcescens*[54], this pigment was not suitable for the development as human therapeutic due to the limited safety of this opportunistic human pathogen. Since *Streptomyces* fermentations are not associated with endotoxins and other pyrogenic molecules, the UP obtained in this study was deemed as safe for human therapy and suitable for development as novel anticancer agent.

Before *in vivo* studies could be performed, it was important to demonstrate the functional activity of UP-Au nanoparticles and whether the nano-packing influenced *in vitro* anticancer activity

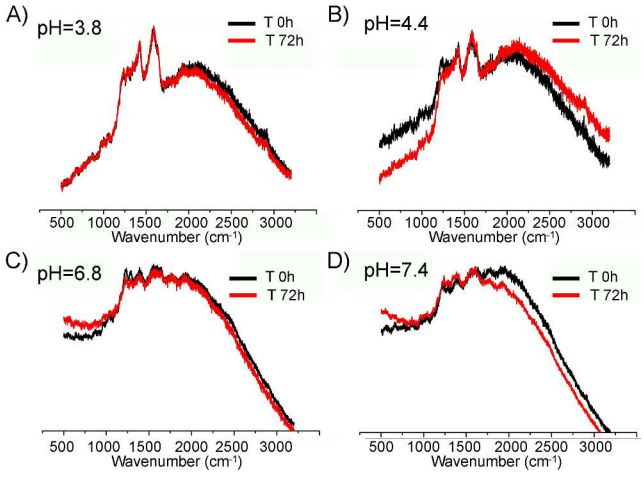

Fig.3 Raman spectra of UP-Au incubated for 72 h in Glycine-HCl buffer pH 3.8 (A), Glycine-HCl buffer pH 4.4 (B) MES buffer pH 6.2 (C) and HEPES buffer pH 7.4 (D).

Table 1 UP and UP-Au mediated cancer cell growth inhibition. Values show concentrations (μg/ml) at which 50% cell growth inhibition occurs (IC_{50}).

	UP		UP[a] within conjugate		UP-Au	
Assay	MTT	CV	MTT	CV	MTT	CV
A549 (Lung)	0.5 ± 0.1[b]	2.2 ± 0.5	0.4 ± 0.1	0.6 ± 0.1	4.4 ± 0.6	6.0 ± 1
A375 (Melanoma)	0.5 ± 0.1	3.8 ± 0.8	2.2 ± 0.1	2.7 ± 0.4	24 ± 1	29 ± 1
HCT-116 (Colon)	1.0 ± 0.1	3.6 ± 0.1	2.0 ± 0.2	2.6 ± 0.1	22 ± 2	26 ± 1
MCF-7 (Breast)	3.4 ± 0.3	3.6 ± 0.4	3.5 ± 0.3	4.0 ± 0.2	38 ± 3	40 ± 2

[a] IC_{50} values calculated with respect to the amount of UP within nano-preparation; [b] IC_{50} values are calculated from three independent experiments and are expressed as means ± SD

of UP and its mechanism of action. Therefore we treated four different cancer cell lines with wide range of UP and UP-Au complex doses for 48 h and the viability was assessed by MTT and CV tests (Table 1). We have included both viability screens MTT (indicating number of metabolically active cells) and CV (indicating total number of live adherent cells) as from the result agreement conclusion can be drawn if the mitochondria were the initial target of the tested compound. Obtained results showed that all tested cell lines were sensitive to both treatments (UP and UP-Au) with the inhibitory concentrations at 50% effect level (IC_{50}) being between 0.5- 4 μg/ml for pure UP, and between 4-40 μg/ml when the UP conjugated to Au nanoparticles (UP-Au) was applied (Table 1). Previously UP isolated from *S. marcescens* has been shown to efficiently kill breast cancer cells, P388 leukemia cells, as well as lung and human hepatic carcinoma cells.[8-10] Cytotoxicity was related to the presence of methoxy group (Fig. 1A) of UP.[55, 56] IC_{50} values obtained in these studies are in a good agreement with our findings. Ho and coworkers reported IC_{50} values of UP between 3.25 to 8.57 μM against several breast cancer cell lines.[10] In our study IC_{50} values for MCF-7 cells were approximately 9 μM (Table 1). In addition this is the first report showing that UP decreased the viability of melanoma and human colon cancer cells.

Almost 10-fold difference in the IC_{50} between pure UP and nano-preparation was consistent with the amount of UP within conjugate (10% w/w; Supporting Information, Fig. S1). To further examine whether the observed activity was due to the UP an appropriate control cell treatment with naked Au nanoparticles was also carried out revealing that 55 μg/ml of Au had almost no influence on cell viability of A375, HCT-116 and MCF-7 (Supporting Information, Fig. S2), confirming that cytotoxicity was associated with the methoxy group of UP. Gold nanoparticles at this concentration caused 80% killing of A549 cells suggesting the unsuitability of this cell line for further studies using the conjugation approach.

In the case of UP there was a discrepancy between the IC_{50} values of the pigment calculated from MTT and CV tests, with IC_{50} values obtained by CV test being 4.4-, 7.6- and 3.6-fold higher for A549, A375 and HCT-116 cell lines respectively in comparison to MTT values (Table 1) indicating that UP targets mitochondrial respiration of the cells which precedes the cell dying. Therefore, IC_{50} values obtained by CV test were taken as more relevant for estimation of UP's efficacy. In the case of MCF-7 cell line IC_{50} values from both tests were comparable indicating different mechanism of action. This was also the case when UP-Au was applied as IC_{50} values calculated from both tests were in good agreement for all cell lines tested (Table 1).
Comparison of the cytotoxicity of biologically active UP and UP within UP-Au complex revealed that conjugation of UP with Au nanoparticles slightly potentiated the efficiency of the pigment that was estimated from the IC_{50} values obtained by CV test (Table 1). Gold nano-packing is usually associated with improved cellular uptake thus increased *in vitro* cytotoxicity[24], however this effect depends on the cancer cell line.Reduction of IC_{50} values of 1.7-fold was observed for A549 and the reduction of 1.4-fold for A375 and HCT-116 cell lines while the conjugation caused slight decrease of UP efficiency in the case of MCF-7 cell line (Table 1). Differential cancer cell lines responses indicated degree of specificityof UP-Au complex. Interestingly, Brown and coworkers reported 1.3 to 5.7-fold improvement when oxaliplatin was conjugated to Au nanoparticles but no change was observed in the case of HCT-116 cells.[31]

3.4 Cytotoxicity of UP on HCT-116 colon cancer cell line

Based on the cytotoxicity screen and considering the resistance to most of the known anticancer therapeutics including resistance to

Cite this: DOI: 10.1039/c0xx00000x

www.rsc.org/xxxxxx

ARTICLE TYPE

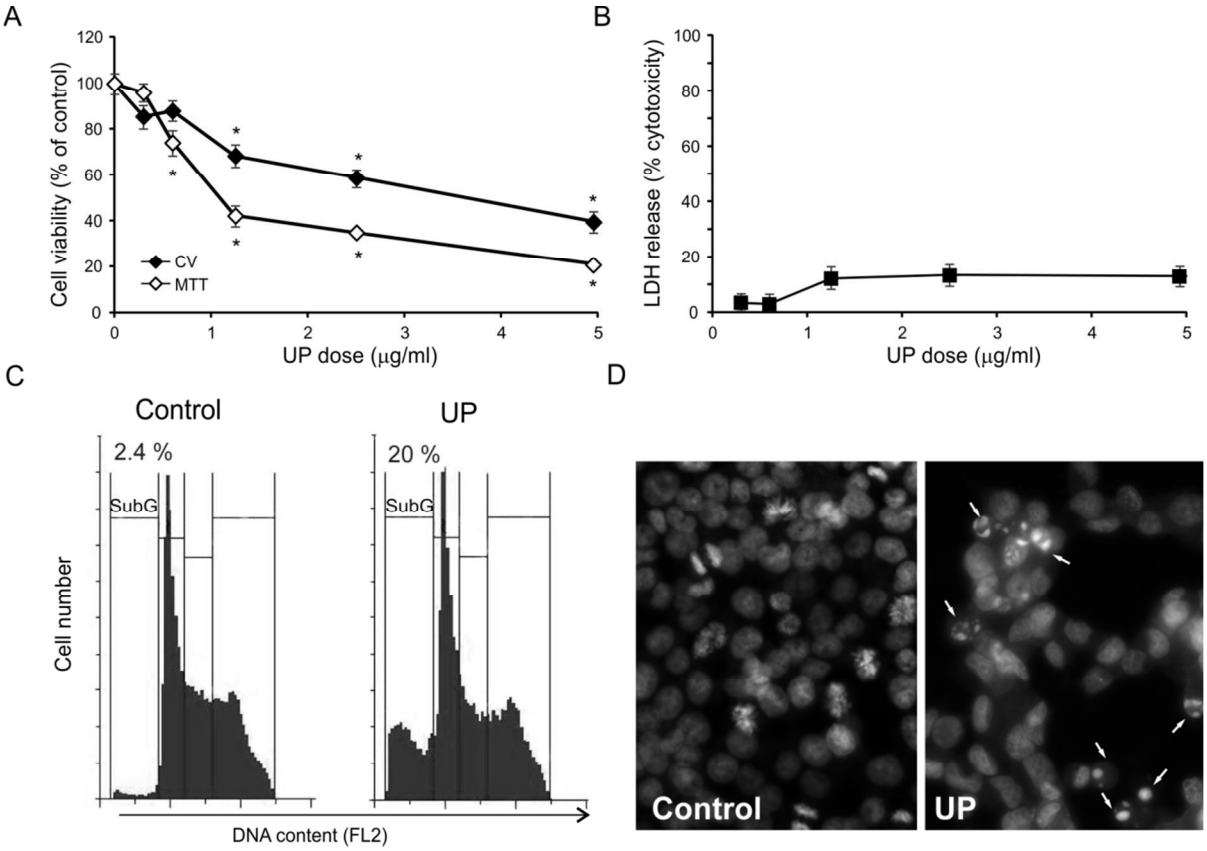

Fig.4 UP induced apoptosis in HCT-116 cells. Cellswere treated with a range of concentrations of UP for 48 h, after which cell viability was determined by MTT and CV assays (A) and LDH release was assessed (B). The data are presented as mean ± SD from representative of three independent experiments, p* <0.05 refers to untreated cultures. Cells cultured in medium without treatment (control) or in the presence of IC_{50} of UP (3.6 μg/ml) for 48 h were stained by PI and cell cycle distribution was analyzed by flow cytometry (C) and cells were visualized by a fluorescent microscope (D). Arrows within micrograph indicate apoptotic cells with condensed chromatin and apoptotic bodies.

cisplatin, the human colon cancer HCT-116 cell line was selected for further studies. UP showed dose-dependent activity on HCT-116 cells, being cytotoxic already at concentration of 1 μg/ml as observed by both MTT and CV assays (Fig. 4A). However, at this concentration the number of viable cells determined by MTT assay was almost 2-fold lower comparing to CV assay results most likely due to the mitochondrial dysfunction caused by UP treatment. The moderate increase of LDH in culture supernatants of 20% was detected only after 48 h upon the treatment with UP concentrations higher than 1 μg/ml, suggesting that necrosis is not the primary cause of the cell death (Fig. 4B).

Cell cycle analysis revealed that the treatment with UP IC_{50} concentration (3.6 μg/ml) caused accumulation of HCT-116 cells in SubG phase (20%) compared to nontreated control (2.4%) indicating apoptotic cell death (Fig 4C). Consistently, exposure to UP at this concentration resulted in accumulation of hypodiploid cells with typical morphological signs of apoptosis such as condensed chromatin, decreased volume of nuclei and numerous apoptotic bodies as observed by fluorescent microscopy of PI stained cells (Fig. 4D). It is worth mentioning that in UP treated cells apoptosis could not be analysed by Annexin V/PI double staining and flow-cytometry due to its autoflorescence (data not shown).[38]

3.5 Cytotoxicity of UP-Au complex on HCT-116 colon cancer cell line

The dose dependent activity of UP-Au complex was observed on HCT-116 cells (Fig. 5A). Notably, opposite to UP treatment, no difference was observed in the cell viability when the two viability assays were used indicating that UP in conjugated form realized its cytotoxicity through the different mechanisms than UP alone (Fig. 5A). Measuring of LDH release in the supernatant after 48 h of treatment with UP-Au showed the absence of necrosis at all tested concentrations (Fig. 5B).

Cells were also cultivated in the presence of IC_{50} dose of UP-Au (26 μg/ml) for 48 h when the apoptotic cell death was examined by different methods. Flow cytometric analysis of Annexin V/PI double staining of UP-Au conjugate -treated cells revealed that the complex induced apoptosis in 47% of treated cells (Fig. 5C). 35% of UP-Au treated cells were only Annexin V

Cite this: DOI: 10.1039/c0xx00000x

www.rsc.org/xxxxxx

ARTICLE TYPE

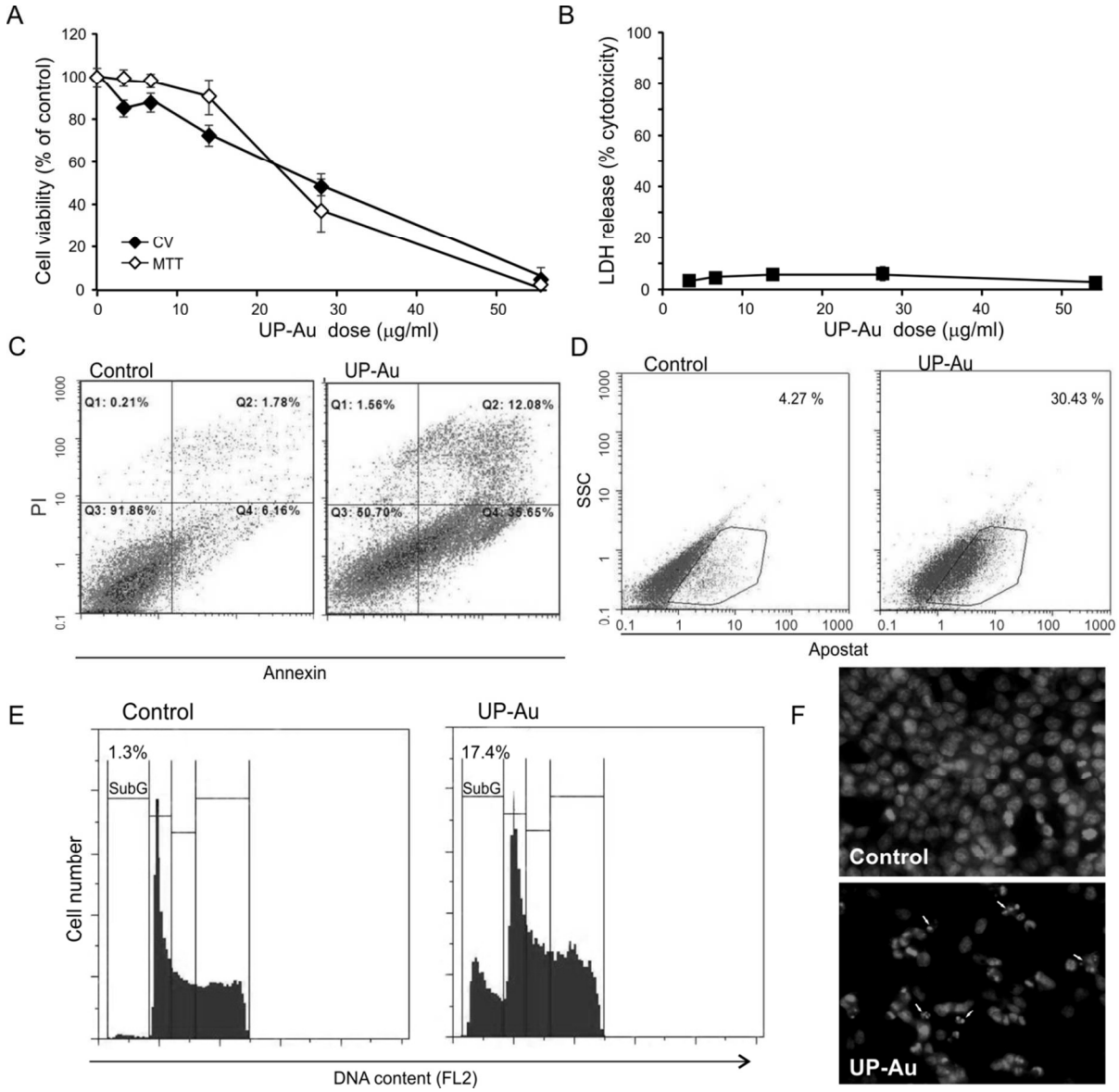

Fig.5 UP-Au induces caspase-dependent apoptosis in HCT-116 cells. Cellswere treated with a range of UP-Au concentrations for 48 h, after which cell viability was determined by MTT and CV assays (A) and LDH release was assessed (B). Data is an average of three independent determinations. After the treatment with IC_{50} ofUP-Au conjugate (26 μg/ml) for 48 h cells were stained with Annexin V and PI (C) or Apostat (D) and then analysed by flow cytometry. Analysis of cell cycle distribution of PI stained cells by flow cytometry (E) and fluorescent microscopy (F). Arrows within micrograph indicate apoptotic cells with condensed chromatin and apoptotic bodies. Cells cultured in medium without treatment were used as a control.

positive indicating early apoptosis and 12% of cells were positive for both Annexin V/PI staining showing late phase of this process (Fig. 5C). The exposure to UP-Au caused remarkable activation of caspases as detected by increase of Apostat positive cells (Fig. 5D) with further DNA fragmentation observed by both cell cycle analysis and PI staining (Fig. 5E and 5F). Similarly to UP treatment, UP-Au conjugate caused 10- fold higher accumulation of cells in SubG phase (Fig. 5E) with accumulation of apoptotic bodies observed by fluorescent microscopy (Fig. 5F). Together these results demonstrate that caspase dependent apoptosis is leading mechanism of UP-Au's tumoricidal activity.

3.6 Mechanism of UP and UP-Au tumoricidal action in colon cancer cells

Initial indications of the mitochondrial involment in UP cytotoxicity obtaind from the cell viability studies were confirmed by the detection of mitochondria membrane potential changes in HCT-116 cells upon UP treatment (Fig. 6).

Interestingly, this mitochondrial membrane depolarisation was not detected upon treatment with UP-Au indicating that binding of UP to gold changed intracellular pathways involved in the realization of apoptosis.

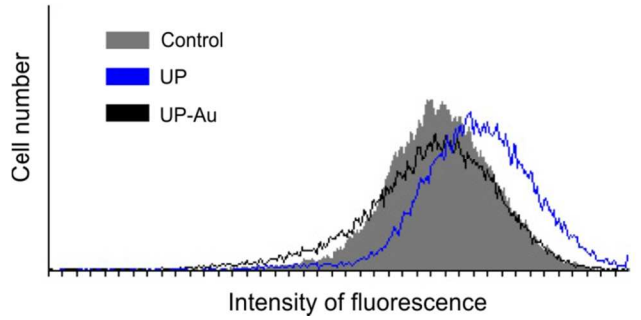

Fig.6 UP induced mitochondrial membrane depolarization. The change in mitochondrial membrane potential was detected after UP and UP-Au treatments with IC_{50} for 48 h followed by JC1 staining and analysed by flow cytometry. Nontreated cells were used as a control.

Reports on nano-packing influencing the mechanism of activity of conjugated drugs are scarce. To further address this, the expression of mitochondrial apoptotic pathway proteins Bim, Smac/Diablo and XIAP were also monitored. The expression of pro-apoptotic marker Bim was upregulated upon UP treatment. Contrary, treatment with UP-Au transiently inhibited its expression during the 24 h (Fig. 7A and 7D). Upregulation of Smac/Diablo triggered by UP was not observed upon conjugation with gold (Fig. 7C and 7D). On the other hand both treatments inhibited XIAP in similar manner (Fig. 7B and 7D).

Taken together, our results demonstrate that conjugation of UP with gold nanoparticles preserved its anticancer activity, but converted the intracellular signals from mitochondrial dependent to mitochondrial independent apoptotic process. Low expression of Bim could be of remarkable importance for this event. It is well known that Bim is sequestered in the microtubule-associated dyeing motor complex.[57] Dissociation of Bim from this complex in response to toxic stimuli, enable it to interact with and inactivate Bcl-2, thereby enhancing apoptosis through forcing of mitochondrial PTP formation. According to this, decreased level of Bim indicated increase of free Bcl-2 that prevented mitochondrial membrane disruption, further documented by the absence of SMAC/DIABLO release within first 24 h of exposure to UP-Au. On the other hand, it is possible that nano-packing of UP promoted receptor dependent apoptotic signal, without its amplification through mitochondrial loop. Moreover, this indicated less general toxicity of the compound coupled with Au that, together with stabilization could be a great advantage of this approach in UP application.

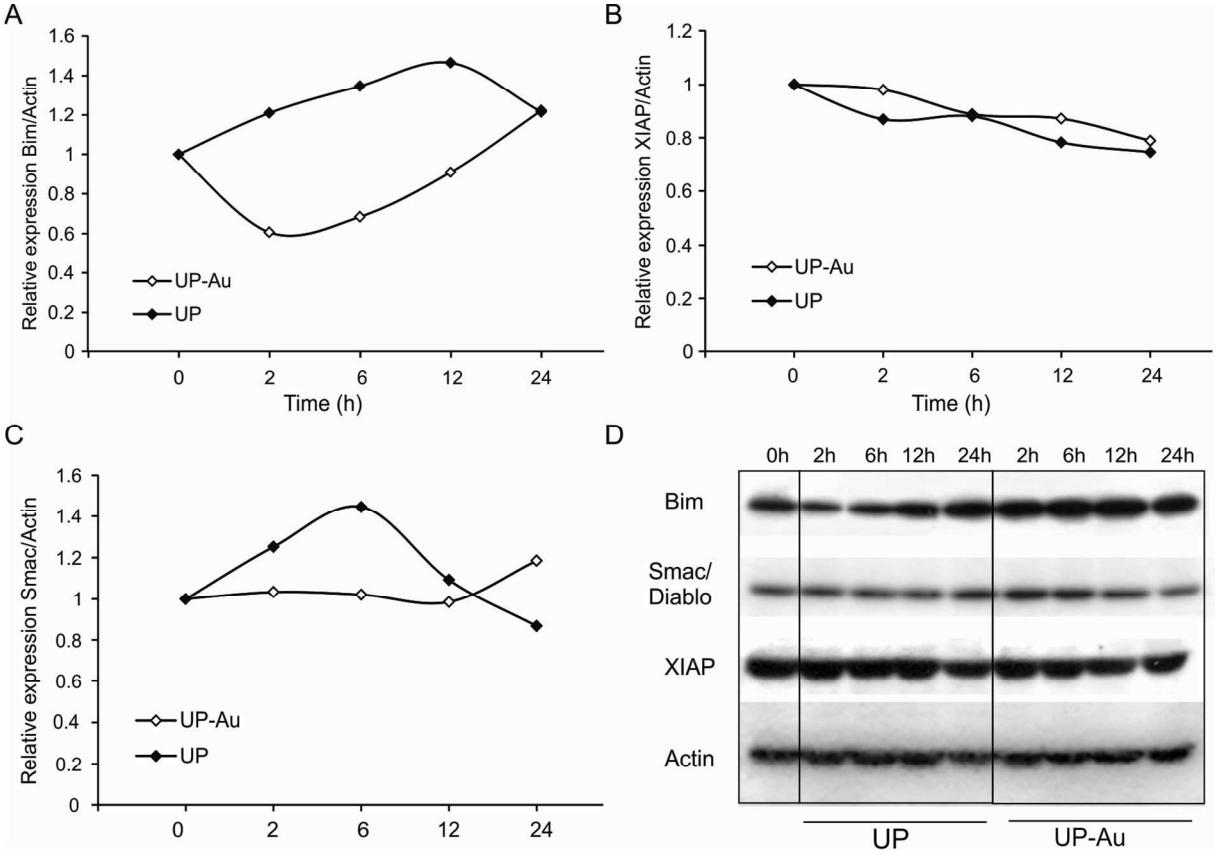

Fig.7 UP-Au causes apoptosis of colon cancer cells independent of mitochondrial pathway. HCT-116 cells were treated with IC_{50} concentrations of UP or UP-Au and WB was performed using antibodies specific for different components of mitochondrial cell death pathway: Bim (A, D), XIAP (B, D), Smac (C, D). Values in A, B and C present the amounts of specific proteins in relation to actin expression obtained after quantification of chemiluminescence.

Cite this: DOI: 10.1039/c0xx00000x

www.rsc.org/xxxxxx

ARTICLE TYPE

Conclusions

Considering global incidence of colon cancer and prominent resistance to therapeutics, the development of efficient colon cancer drug is still a challenging task. Undecylprodigiosin was determined to effectively cause apoptosis of colon cancer cells. Indeed, this molecule is promising lead molecule for cancer therapy. As a result of multistep chemical synthesis efforts an UP derivative (PNU-156804) reached preclinical trials.[58] In this study nano-packing of biotechnologically obtained UP was identified as suitable route towards new formulations of UP with increased stability and improved activity. The conjugation of UP to Au nanoparticles resulted in modulation of the mechanism of its activity as well. The inherent versatility of gold nanoparticles as well as the available selection of linkers means that diverse family of UP-Au conjugates can be produced to tune and improve this approach.

The most of conventional anticancer drugs such as platinum based drugs, 5-fluorouracil, doxorubicin and methotrexate, induce cancer cell apoptosis through activation of mitochondrial cell death pathway [59] and therefore show less specific activity. Combination therapy of these drugs with UP-Au could lead to improved efficiency of the treatments and reduced side effects.

Future work will focus on an *in vivo* setting to establish UP-based drug toxicity and anti-tumor efficacy as well as further development of UP-Au complexes by including various drug combinations and/or involving targeting molecules for the cancer-specific delivery.

Acknowledgements

Part of the work performed at the University of Belgrade, Institute of Molecular Genetics and Genetic Engineering and Institute for Biological Research “Sinisa Stankovic” was supported by the Ministry of Education, Science and Technological Development of Serbia (Project No. 173048 and 173013). Part of the work performed at Argonne National Laboratory was supported by the U.S. Department of Energy, Office of Science, Office of Basic Energy Sciences, under Contract DE-AC02-06CH11357.

Notes and references

[a] *University of Belgrade, Institute of Molecular Genetics and Genetic Engineering, VojvodeStepe 444a, P.O.Box 23, 11010 Belgrade, Serbia*
[b] *Institute for Biological Research "SinisaStankovic", Department of Immunology, University of Belgrade, BulevarDespotaStefana 142, 11060 Belgrade, Serbia*
[c] *Materials Science Division, Argonne National Laboratory, 9700 South Cass Avenue, Argonne, Illinois 60439, United States*
[#] Authors JNR, MM and YK contributed equally to this work.
**** Corresponding Authors:***
Lidija Senerovic Tel.: + 381 11 3976 034; Fax.: + 381 11 3975 808; E-mail: seneroviclidija@imgge.bg.ac.rs
Vojislav Stamenkovic Tel.: + 1 630 252 8946; Fax.:+1 630 252 7777 ; E-mail: vrstamenkovic@anl.gov

† Electronic Supplementary Information (ESI) available: [TGA analysis of UP conjugated Au nanoparticles; Naked Au nanoparticles mediated cancer cell growth inhibition estimated by MTT and CV assays].

1. L. Kelland, *Nat Rev Cancer*, 2007, **7**, 573-584.
2. B. C. Baguley, *Mol Biotechnol*, 2010, **46**, 308-316.
3. G. M. Cragg, P. G. Grothaus and D. J. Newman, *Chem Rev*, 2009, **109**, 3012-3043.
4. N. R. Williamson, P. C. Fineran, T. Gristwood, S. R. Chawrai, F. J. Leeper and G. P. Salmond, *Future Microbiol*, 2007, **2**, 605-618.
5. K. Papireddy, M. Smilkstein, J. X. Kelly, Shweta, S. M. Salem, M. Alhamadsheh, S. W. Haynes, G. L. Challis and K. A. Reynolds, *J Med Chem*, 2011, **54**, 5296-5306.
6. D. Kim, J. S. Lee, Y. K. Park, J. F. Kim, H. Jeong, T. K. Oh, B. S. Kim and C. H. Lee, *J Appl Microbiol*, 2007, **102**, 937-944.
7. N. Stankovic, V. Radulovic, M. Petkovic, I. Vuckovic, M. Jadranin, B. Vasiljevic and J. Nikodinovic-Runic, *Appl Microbiol Biotechnol*, 2012, **96**, 1217-1231.
8. R. Liu, C. B. Cui, L. Duan, Q. Q. Gu and W. M. Zhu, *Arch Pharm Res*, 2005, **28**, 1341-1344.
9. P. Liu, Y. Y. Wang, X. Qi, Q. Gu, M. Geng and J. Li, *PLoS One*, 2013, **8**, e65381.
10. T. F. Ho, C. J. Ma, C. H. Lu, Y. T. Tsai, Y. H. Wei, J. S. Chang, J. K. Lai, P. J. Cheuh, C. T. Yeh, P. C. Tang, J. Tsai Chang, J. L. Ko, F. S. Liu, H. E. Yen and C. C. Chang, *Toxicol Appl Pharmacol*, 2007, **225**, 318-328.
11. M. E. Davis, Z. G. Chen and D. M. Shin, *Nat Rev Drug Discov*, 2008, **7**, 771-782.
12. Z. Cheng, A. Al Zaki, J. Z. Hui, V. R. Muzykantov and A. Tsourkas, *Science*, 2012, **338**, 903-910.
13. J. L. Markman, A. Rekechenetskiy, E. Holler and J. Y. Ljubimova, *Adv Drug Deliv Rev*, 2013.
14. J. M. Bergen, H. A. von Recum, T. T. Goodman, A. P. Massey and S. H. Pun, *Macromol Biosci*, 2006, **6**, 506-516.
15. X. D. Zhang, H. Y. Wu, D. Wu, Y. Y. Wang, J. H. Chang, Z. B. Zhai, A. M. Meng, P. X. Liu, L. A. Zhang and F. Y. Fan, *Int J Nanomedicine*, 2010, **5**, 771-781.
16. E. E. Connor, J. Mwamuka, A. Gole, C. J. Murphy and M. D. Wyatt, *Small*, 2005, **1**, 325-327.
17. C. R. Patra, R. Bhattacharya, E. Wang, A. Katarya, J. S. Lau, S. Dutta, M. Muders, S. Wang, S. A. Buhrow, S. L. Safgren, M. J. Yaszemski, J. M. Reid, M. M. Ames, P. Mukherjee and D. Mukhopadhyay, *Cancer Res*, 2008, **68**, 1970-1978.
18. W. Liu, X. Li, Y. S. Wong, W. Zheng, Y. Zhang, W. Cao and T. Chen, *ACS Nano*, 2012, **6**, 6578-6591.
19. A. Dong, X. Ye, J. Chen, Y. Kang, T. Gordon, J. M. Kikkawa and C. B. Murray, *Journal of the American Chemical Society*, 2011, **133**, 998-1006.

20. X. Ye, L. Jin, H. Caglayan, J. Chen, G. Xing, C. Zheng, D.-N. Vicky, Y. Kang, N. Engheta, C. R. Kagan and C. B. Murray, *Acs Nano*, 2012, **6**, 2804-2817.
21. L. Brannon-Peppas and J. O. Blanchette, *Adv Drug Deliv Rev*, 2004, **56**, 1649-1659.
22. S. Hirn, M. Semmler-Behnke, C. Schleh, A. Wenk, J. Lipka, M. Schaffler, S. Takenaka, W. Moller, G. Schmid, U. Simon and W. G. Kreyling, *Eur J Pharm Biopharm*, 2011, **77**, 407-416.
23. S. D. Perrault, C. Walkey, T. Jennings, H. C. Fischer and W. C. Chan, *Nano Lett*, 2009, **9**, 1909-1915.
24. L. Vigderman and E. R. Zubarev, *Adv Drug Deliv Rev*, 2013, **65**, 663-676.
25. A. Shapira, Y. D. Livney, H. J. Broxterman and Y. G. Assaraf, *Drug Resist Updat*, 2011, **14**, 150-163.
26. S. Aryal, J. J. Grailer, S. Pilla, D. A. Steeber and S. Q. Gong, *J Mater Chem*, 2009, **19**, 7879-7884.
27. F. Wang, Y. C. Wang, S. Dou, M. H. Xiong, T. M. Sun and J. Wang, *ACS Nano*, 2011, **5**, 3679-3692.
28. X. Dong and R. J. Mumper, *Nanomedicine (Lond)*, 2010, **5**, 597-615.
29. D. N. Heo, D. H. Yang, H. J. Moon, J. B. Lee, M. S. Bae, S. C. Lee, W. J. Lee, I. C. Sun and I. K. Kwon, *Biomaterials*, 2012, **33**, 856-866.
30. E. C. Dreaden, S. C. Mwakwari, Q. H. Sodji, A. K. Oyelere and M. A. El-Sayed, *Bioconjug Chem*, 2009, **20**, 2247-2253.
31. S. D. Brown, P. Nativo, J. A. Smith, D. Stirling, P. R. Edwards, B. Venugopal, D. J. Flint, J. A. Plumb, D. Graham and N. J. Wheate, *Journal of the American Chemical Society*, 2010, **132**, 4678-4684.
32. M. Prabaharan, J. J. Grailer, S. Pilla, D. A. Steeber and S. Gong, *Biomaterials*, 2009, **30**, 6065-6075.
33. C. M. Shen, C. Hui, T. Z. Yang, C. W. Xiao, J. F. Tian, L. H. Bao, S. T. Chen, H. Ding and H. J. Gao, *Chem Mater*, 2008, **20**, 6939-6944.
34. C. B. Murray, C. R. Kagan and M. G. Bawendi, *Annu Rev Mater Sci*, 2000, **30**, 545-610.
35. Y. Kang, M. Li, Y. Cai, M. Cargnello, R. E. Diaz, T. R. Gordon, N. L. Wieder, R. R. Adzic, R. J. Gorte, E. A. Stach and C. B. Murray, *Journal of the American Chemical Society*, 2013, **135**, 2741-2747.
36. L. E. Mihajlovic, A. Savic, J. Poljarevic, I. Vuckovic, M. Mojic, M. Bulatovic, D. Maksimovic-Ivanic, S. Mijatovic, G. N. Kaluderovic, S. Stosic-Grujicic, D. Miljkovic, S. Grguric-Sipka and T. J. Sabo, *J Inorg Biochem*, 2012, **109**, 40-48.
37. S. Mijatovic, D. Maksimovic-Ivanic, J. Radovic, D. Miljkovic, G. N. Kaludjerovic, T. J. Sabo and V. Trajkovic, *Cell Mol Life Sci*, 2005, **62**, 1275-1282.
38. E. Tenconi, P. Guichard, P. Motte, A. Matagne and S. Rigali, *J Microbiol Methods*, 2013, **93**, 138-143.
39. S. Mo, B. S. Kim and K. A. Reynolds, *Chem Biol*, 2005, **12**, 191-200.
40. S. W. Tsao, B. A. Rudd, X. G. He, C. J. Chang and H. G. Floss, *J Antibiot (Tokyo)*, 1985, **38**, 128-131.
41. G. Sonavane, K. Tomoda and K. Makino, *Colloids Surf B Biointerfaces*, 2008, **66**, 274-280.
42. Y. Pan, S. Neuss, A. Leifert, M. Fischler, F. Wen, U. Simon, G. Schmid, W. Brandau and W. Jahnen-Dechent, *Small*, 2007, **3**, 1941-1949.
43. P. Ghosh, G. Han, M. De, C. K. Kim and V. M. Rotello, *Adv Drug Deliv Rev*, 2008, **60**, 1307-1315.
44. H. Maeda, J. Wu, T. Sawa, Y. Matsumura and K. Hori, *J Control Release*, 2000, **65**, 271-284.
45. I. Hussain, S. Graham, Z. Wang, B. Tan, D. C. Sherrington, S. P. Rannard, A. I. Cooper and M. Brust, *J Am Chem Soc*, 2005, **127**, 16398-16399.
46. J. Kimling, M. Maier, B. Okenve, V. Kotaidis, H. Ballot and A. Plech, *J Phys Chem B*, 2006, **110**, 15700-15707.
47. X. C. Ye, J. Chen and C. B. Murray, *Journal of the American Chemical Society*, 2011, **133**, 2613-2620.
48. L. Polavarapu, N. Venkatram, W. Ji and Q. H. Xu, *ACS Appl Mater Interfaces*, 2009, **1**, 2298-2303.
49. J. W. Bennett and R. Bentley, *Adv Appl Microbiol*, 2000, **47**, 1-32.
50. A. Furstner, J. Grabowski, C. W. Lehmann, T. Kataoka and K. Nagai, *Chembiochem*, 2001, **2**, 60-68.
51. N. R. Williamson, P. C. Fineran, F. J. Leeper and G. P. Salmond, *Nat Rev Microbiol*, 2006, **4**, 887-899.
52. G. E. Craig, S. D. Brown, D. A. Lamprou, D. Graham and N. J. Wheate, *Inorg Chem*, 2012, **51**, 3490-3497.
53. J. Regourd, A. A. Ali and A. Thompson, *J Med Chem*, 2007, **50**, 1528-1536.
54. Y. H. Wei, W. J. Yu and W. C. Chen, *J Biosci Bioeng*, 2005, **100**, 466-471.
55. B. Montaner and R. Perez-Tomas, *Curr Cancer Drug Targets*, 2003, **3**, 57-65.
56. R. Perez-Tomas, B. Montaner, E. Llagostera and V. Soto-Cerrato, *Biochem Pharmacol*, 2003, **66**, 1447-1452.
57. H. Puthalakath, D. C. Huang, L. A. O'Reilly, S. M. King and A. Strasser, *Mol Cell*, 1999, **3**, 287-296.
58. S. M. Stepkowski, Z. S. Nagy, M. E. Wang, F. Behbod, R. Erwin-Cohen, B. D. Kahan and R. A. Kirken, *Transplant Proc*, 2001, **33**, 3272-3273.
59. K. Hara, E. Kasahara, N. Takahashi, M. Konishi, J. Inoue, M. Jikumaru, S. Kubo, H. Okamura, E. Sato and M. Inoue, *J Pharmacol Exp Ther*, 2011, **337**, 838-845.

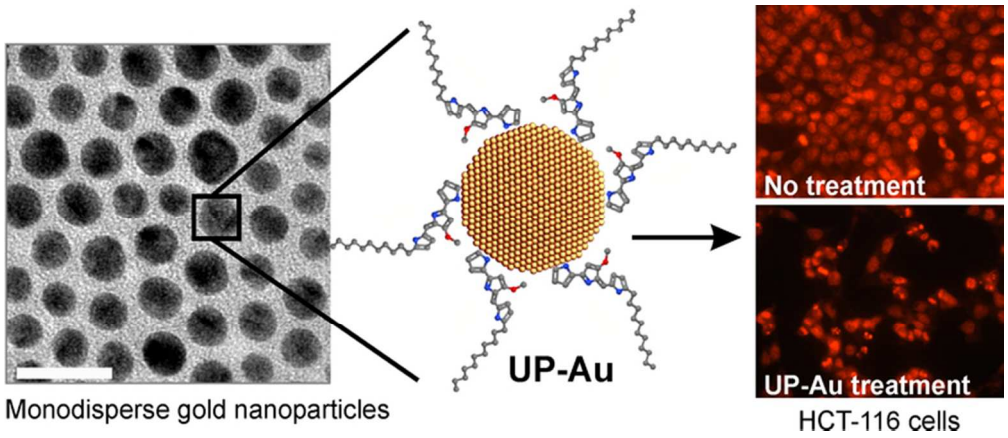

Bacterial pigment undecylprodigiosin was conjugated to monodisperse gold nanoparticles resulting in improved stability and cytotoxicity against colon cancer cells.
34x14mm (600 x 600 DPI)

Bacterial pigment undecylprodigiosin was conjugated to monodisperse gold nanoparticles resulting in improved stability and cytotoxicity against colon cancer cells.